Available online at www.sciencedirect.com
SCIENCE DIRECT®
Biochemical Pharmacology 67 (2004) 927–935
Biochemical Pharmacology
www.elsevier.com/locate/biochempharm

Disorazol A_1, a highly effective antimitotic agent acting on tubulin polymerization and inducing apoptosis in mammalian cells

Yasser A. Elnakady[a], Florenz Sasse[a,*], Heinrich Lünsdorf[b], Hans Reichenbach[a]

[a]*Department of Natural Product Biology, GBF, German Research Centre for Biotechnology, D-38124 Braunschweig, Germany*
[b]*Division of Microbiology, GBF, German Research Centre for Biotechnology, D-38124 Braunschweig, Germany*

Received 13 June 2003; accepted 15 October 2003

Abstract

Disorazol A_1, a macrocyclic polyketide compound that is produced by the myxobacterium *Sorangium cellulosum* showed a remarkably high cytostatic activity. It inhibited the proliferation of different cancer cell lines including a multidrug-resistant KB line at low picomolar levels. In presence of disorazol A_1, the nuclei of the cells increased in size and the cells often became multinucleate. Low concentrations of disorazol (<100 pM) induced an apoptotic process, characterized by enhanced capase-3 activity and DNA laddering, and abnormal, multipolar mitotic spindles. Low concentrations also induced an accumulation of p53 protein in the nucleus. At higher concentrations, we observed an accumulation of the cells in the G_2/M-phase of the cell cycle, and a depletion of microtubules. *In vitro*, disorazol A_1 inhibited the polymerization of tubulin in a concentration-dependent manner and independently of microtubule-associated proteins. Correspondingly it induced a complete depolymerization of microtubules prepared *in vitro*. Formation of defined degradation structures was not observed. Disorazol is a novel, highly effective antimitotic agent. Efforts are going on to develop it as an anticancer drug.

Keywords: Disorazol; Microtubules; Tubulin; Apoptosis; p53; Multinucleate cells

1. Introduction

Natural products are an unsurpassed source of novel chemotherapeutic drugs. Tubulin-interacting compounds, such as vinblastine and paclitaxel, cause cells to accumulate in the M-phase of the cell cycle through inhibition of mitosis. Microtubules are highly dynamic polymeric structures of tubulin, which are involved in many cellular activities including maintenance of cell structure, cellular transport, and cell proliferation [1]. Microtubular function depends on these dynamics, which is especially high during formation of the mitotic spindle. Interfering with microtubular dynamics of the mitotic spindle is the basis for the anticancer activities of drugs that either inhibit the polymerization of microtubules, e.g. *Vinca* alkaloids, or promote it, e.g. taxanes.

As these compounds induce a fragmentation of the nuclei which can easily be shown by DAPI staining, we used a microtiterplate assay with L929 mouse cells in order to screen small amounts of myxobacteria grown on agar plates for this effect.[1] The active principle of some positive samples of *Sorangium cellulosum* was shown to be disorazol A_1, a macrocyclic polyketide (Fig. 1), which had been reported as a highly cytotoxic compound with strong antifungal, but no antibacterial activity [2]. Disorazol A_1 was the main compound among twenty-nine disorazols that were isolated from *S. cellulosum*, strain So ce12 [3]. The disorazols are macrocyclic dilactones of 2-pentadecyloxazole-4-carboxylic acids.

Here we show that disorazol A_1 is an antimitotic compound that interferes with microtubule formation, blocks mitosis, and induces apoptosis.

2. Materials and methods

2.1. Natural compounds

Disorazol A_1 and epothilone B were kindly provided from the Division of Natural Product Research at the GBF. Vinblastine was from Sigma.

* Corresponding author. Tel.: +49-531-6181-434; fax: +49-531-6181-395.
E-mail address: fsa@gbf.de (F. Sasse).

Abbreviations: Pgp, P-glycoprotein; MTT, 3-[4,5-dimethylthiazol-2-yl]-2,5-diphenyltetrazolium bromide.

[1] Sasse F, unpublished results.

0006-2952/$ – see front matter © 2003 Elsevier Inc. All rights reserved.
doi:10.1016/j.bcp.2003.10.029

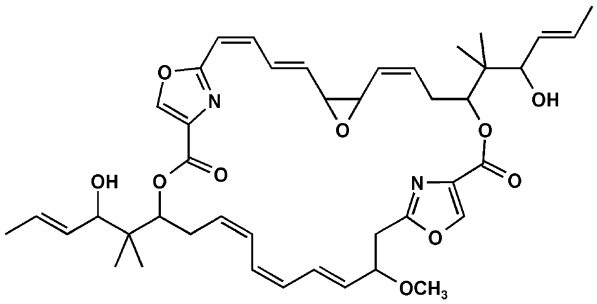

Fig. 1. Chemical structure of disorazol A_1.

2.2. Cell culture and growth inhibition assay

Cell lines were obtained from the American Type Culture Collection (ATCC) and the German Collection of Microorganisms and Cell Cultures (DSMZ). All cell lines were cultivated under conditions recommended by their respective depositors. Cell culture reagents came from Life Technologies Inc. (GIBCO BRL). Plastic ware was from Nunc Inc. Growth inhibition was measured in microtiterplates. Aliquots of 120 μL of the suspended cells (50,000 mL^{-1}) were given to 60 μL of a serial dilution of the inhibitor. After 5 days, growth was determined using the MTT assay [4] or the WST-1 assay (Roche). In order to assay the survival rate, higher cell numbers (250,000 cells/mL) were seeded, and the metabolic activities of the cells monitored over a longer period of time. The absorbance values measured after an incubation with MTT for 2 hr were given as activity parameters.

2.3. Cell cycle analysis

After the appropriate treatment, 10^6 U-937 cells (DSMZ ACC-5) were harvested by centrifugation and then fixed with cold (−20°) 80% methanol. After 30 min of incubation on ice, the cells were washed with PBS (phosphate buffered saline) and then treated with 0.1% saponin in PBS (w/v). Finally 500 μL propidium iodide (20 μg/mL) and RNAse (1 mg/mL) were added, and the cells were incubated at 37° for 30 min. Samples were analyzed by a FacScan (Becton Dickinson Immunocytometry System). Results are presented as the number of cells versus the amount of DNA as indicated by fluorescence intensity.

2.4. Caspase-3 assay

10^6 U-937 cells were extracted with 0.3 mL of 1% Triton X-100 in 10 mM Tris–HCl buffer (pH 7.5) containing 10 mM sodium pyrophosphate and 130 mM NaCl at 4° for 30 min. The cell debris was removed by centrifugation. Fifty microliter aliquots of the cell extract were added to a reaction mixture made of 5 μL of 1 mg/mL Ac-DEVD-AMC (Calbiochem) and 200 μL of 20 mM HEPES (pH 7.5) containing 10% glycerol and 2 mM dithiothreitol in a microtiterplate. After incubation at 37° for 1 hr, the resulting fluorescence was measured with an excitation at 355 nm and emission at 460 nm using a Victor 1420 Multi Label Counter.

2.5. Detection of DNA laddering

DNA of U-937 cells was extracted using a QiAmp DNA mini kit (Qiagen). DNA (1–2 μg) was loaded into a well of a 1.2% agarose gel, separated by electrophoresis at 20 V overnight using TAE buffer (0.04 M Tris–acetate, 1 mM EDTA), and stained by ethidium bromide.

2.6. Cell staining

PtK_2 cells (ATCC CCL-56) were grown on glass coverslips (13 mm diameter) in four-well plates. Exponentially growing cells were incubated with disorazol A_1 for different periods of time. Cells were fixed with cold (−20°) acetone–methanol (1:1) for 10 min. For morphological studies cells were stained by azur B. For labeling the microtubules, cells were incubated with a primary monoclonal antibody against α-tubulin (1:500; Sigma), then with a secondary goat anti-mouse IgG antibody conjugated with Alexa 488 or 594 (1:200; Molecular Probes) at 37° for 45 min. For labeling the centrosomes, we used polyclonal antibodies against γ-tubulin and pericentrin from BAbCO/Covance, and a secondary goat anti-rabbit IgG antibody conjugated with Alexa 594 (Molecular Probes). The nuclei and chromosomes were stained with DAPI (1 μg/mL). In order to investigate p53 localization, we used human A-549 lung carcinoma cells, and anti-p53 monoclonal antibodies (1:500; Transduction Laboratories). The secondary antibody was the same as for microtubule labeling. The cells were washed with PBS between all incubations. The coverslips were mounted using Prolong Antifade (Molecular Probes), and viewed with a Zeiss Axiophot fluorescence microscope using appropriate filter sets.

2.7. Tubulin purification and polymerization assay

Microtubule proteins were purified from porcine brain homogenates using standard procedures that comprise two to three cycles of temperature-dependent polymerization and depolymerization [5]. Microtubule proteins are composed of tubulin and MAPs (microtubule-associated proteins). The purification of tubulin from MAPs was done by phosphocellulose chromatography [6].

Tubulin polymerization was monitored via turbidometry [7]. In the standard polymerization assay, the sample (200 μL of 10–12 μM microtubule proteins) in PEM polymerization buffer (0.1 M PIPES, pH 6.6, 1 mM $MgSO_4$, 1 mM EGTA, and 1 mM GTP) was rapidly warmed to 37° in a water jacketed cuvette holder of a diode array photometer (Beckman Spectrophotometer DU 7500). The absorbance at 350 nm was monitored in absence and presence of the drug.

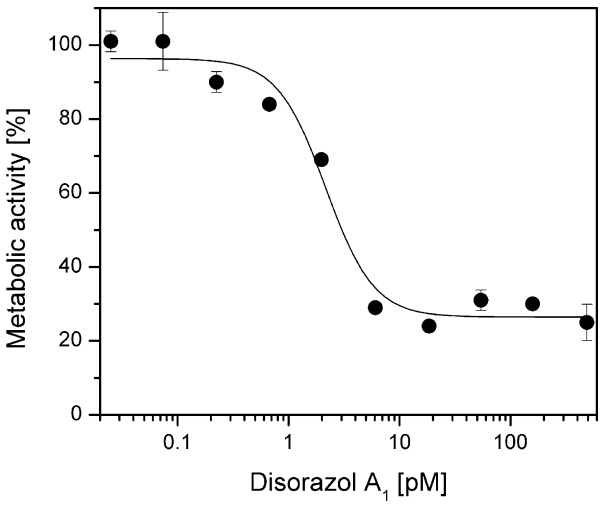

Fig. 2. Concentration-dependent growth inhibition of L929 mouse fibroblasts by disorazol A_1.

2.8. Electron microscopy

Protein samples (5 μL, 10 μM) were adsorbed to carbon-coated copper grids, fixed for 60 s with 0.5% glutaraldehyde in PEM, and then rinsed with distilled water. The grid was negatively contrasted with 2% aqueous uranyl acetate solution, blotted and dried. The specimens were examined under a Zeiss CEM 902 transmission electron microscope.

3. Results

3.1. Inhibition of cell proliferation

Disorazol A_1 (Fig. 1) is an extremely effective inhibitor of mammalian cell proliferation. Fig. 2 shows a concentration-dependent inhibition curve of L929 mouse fibroblasts. The metabolic activity of the cells grown in microtiterplates were measured by an MTT assay after an incubation period of 5 days when the control cells reached confluency. The metabolic activity in each well is dependent on the number of cells that were grown during the 5 days, but also on their vitality. The absorbance values measured with the different disorazol A_1 concentrations were related to control wells whose activities were set to 100%. The activity of the seeded cells accounts to 5%. The sigmoid inhibition curve shows an IC_{50} of 3 pM, and reaches a lower limit at $26 \pm 3\%$, and not 5%, which would be expected when the growth inhibition would be complete. Also at 500 pM, there was an increase in metabolic activity during the 5 days of incubation from 5 to 26%. Microscopic observations and cell counting showed that this increase was due to an increase in cell size, not due to cell proliferation. Experiments with a shorter incubation period (3 days) gave no significantly different results. Disorazol prevents cell proliferation, but has no apparent acute cytotoxic effects. We monitored L929 cells in presence of 13 and 130 pM disorazol A_1 by an MTT assay over a period of 10 days (data not shown). The cells did not propagate under these conditions, showed a slight increase in activity during the first days, which was accompanied by cell enlargement, but no decrease of the metabolic activity, which would be expected with acute cytotoxic effects. In presence of disorazol A_1, the nuclei of the cells increased in size and the cells often became multinucleate as shown in Fig. 3 for PtK_2 cells. The nuclei had irregular shapes and different sizes.

We measured IC_{50} values of several established animal and human tumor cell lines. The data, which are summarized in Table 1, show values between 2 and 42 pmol/L. The high potential of disorazol A_1 becomes especially clear when we compare its data with those of epothilone B and vinblastine, both potent drugs that interfere with microtubular dynamics.

Growth inhibition of the multidrug-resistant cell line KB-V1 was also measured in presence of verapamil. As this compound inactivates the Pgp efflux pump [8], a comparison of the IC_{50} values obtained in presence and in absence of verapamil reveal to which extend disorazol A_1 is pumped out of the cells by the MDR1 Pgp. The data in Table 1 show that disorazol A_1 is a poor substrate of Pgp,

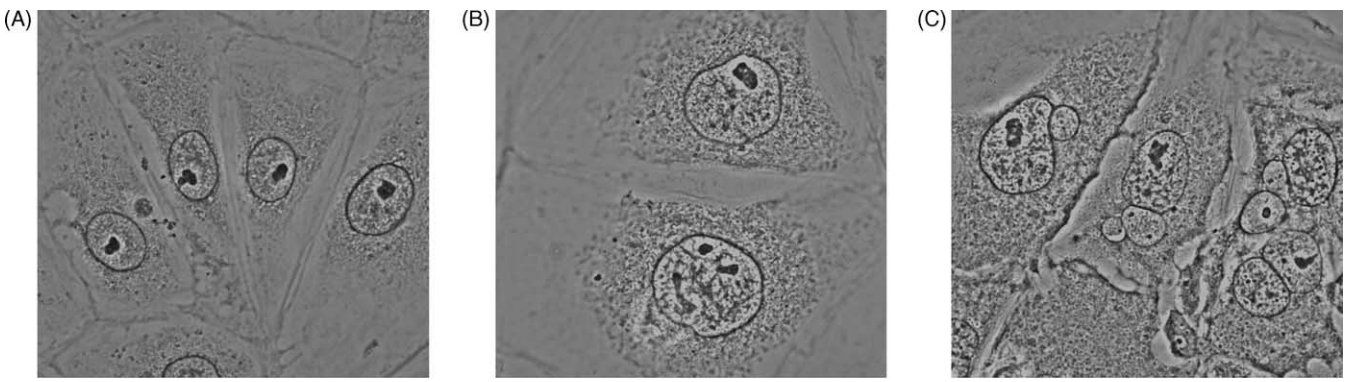

Fig. 3. PtK_2 cells that were incubated with 6.6 pM disorazol A_1 show enlarged nuclei (B) and multinucleate cells (C), which contain nuclei of different size. (A) Untreated control cells. Scale bar: 10 μm.

Table 1
Antiproliferative efficacy of disorazol A_1 against established animal and human tumor cell lines compared with those of epothilone B and vinblastine

Cell line	Origin	IC_{50} (nM)[a]		
		Disorazol A_1	Epothilone B	Vinblastine
L929 (DSMZ ACC-2)	Connective tissue, mouse	0.0038 ± 0.0002 (6)	1.3 ± 0.6 (8)	28 ± 7 (6)
PtK_2 (ATCC CCL-56)	Kidney, potoroo	0.034 ± 0.004 (2)	0.8 ± 0.3 (2)	41 ± 3 (2)
KB-3.1 (DSMZ ACC-158)	Cervix carcinoma, human	0.0025 ± 0.0003 (4)	1.6 ± 0.6 (2)	8.6 ± 0.3 (4)
KB-V1 (DSMZ ACC-149)	Multidrug-resistant KB line	0.042 ± 0.008 (6)	0.57 ± 0.03 (2)	114 ± 31 (4)
KB-V1 (assay in presence of 11 μM verapamil)		0.0040 ± 0.0002 (2)	0.27 ± 0.04 (2)	1.0 ± 0.1 (2)
K-562 (ATCC CCL-243)	Myelogenous leukemia, human	0.006 ± 0.001 (4)	0.69 ± 0.03 (2)	8.7 ± 1.8 (4)
U-937 (DSMZ ACC-5)	Histiocytic lymphoma, human	0.002 ± 0.001 (4)	0.09 ± 0.01 (4)	0.43 ± 0.13 (4)
A-498 (DSMZ ACC-55)	Kidney carcinoma, human	0.016 ± 0.004 (2)	4.3 ± 3.6 (4)	46 ± 12 (2)
A-549 (DSMZ ACC-107)	Lung carcinoma, human	0.0023 ± 0.0005 (2)	0.26 ± 0.14 (2)	5.9 ± 0.5 (2)
SK-OV-3 (ATCC HTB-77)	Adenocarcinoma, ovary, human	0.0049 ± 0.0001 (4)	0.64 ± 0.07 (2)	1.4 ± 0.1 (4)
PC-3 (ATCC CRL-1435)	Adenocarcinoma, prostate, human	0.0071 ± 0.0012 (4)	2.0 ± 0.3 (2)	0.82 ± 0.06 (4)

[a] Arithmetic means ± standard deviation (number of replicates in brackets).

it is transported in a less degree than vinblastine. Epothilone B overcomes MDR1-mediated resistance completely.

3.2. G_2/M blockade of the cell cycle

Cell cycle investigations showed that U-937 cells incubated with disorazol A_1 accumulated in the G_2/M-phase of the cell cycle (Fig. 4). In untreated control cells, only 15% of the whole cell population was in the G_2/M-phase (histogram A), but 85% of the cells had accumulated in this phase when they were incubated with disorazol A_1 (1.3 nM) for 24 hr (histogram B). Only 5% of the cells were in the G_0/G_1-phase. The treated cells also showed a small population of cells with a 4-fold DNA content. This population increased when cells were incubated with the drug for another day (data not shown). An accumulation of cells in the G2/M-phase was also observed at 0.13 nM. G_2/M arrest and an increased population of hyperploid cells was also found with L929 mouse fibroblasts (data not shown).

3.3. Induction of apoptosis

In Fig. 4B, there is also a significant sub-G1 population indicating that an apoptosis is going on. Caspase-3 activity and DNA cleavage are hallmarks of the apoptotic process. Our results showed that caspase-3 activity of treated U-937 cells rapidly increased after the addition of disorazol A_1 reaching a maximum level between 12 and 24 hr (Fig. 5).

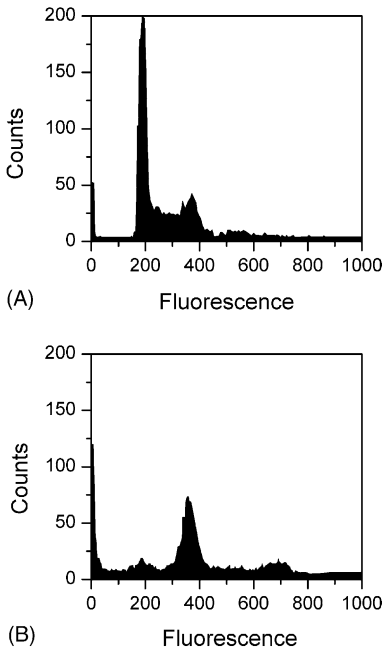

Fig. 4. Histograms of flow cytometry data of U-937 cells. (A) Control cells showed a high peak at G_1-phase. (B) After treatment with disorazol A_1 (1.3 nM) for 24 hr, the cells accumulated in G_2/M-phase. In addition, there is a small cell population with 4-fold DNA content.

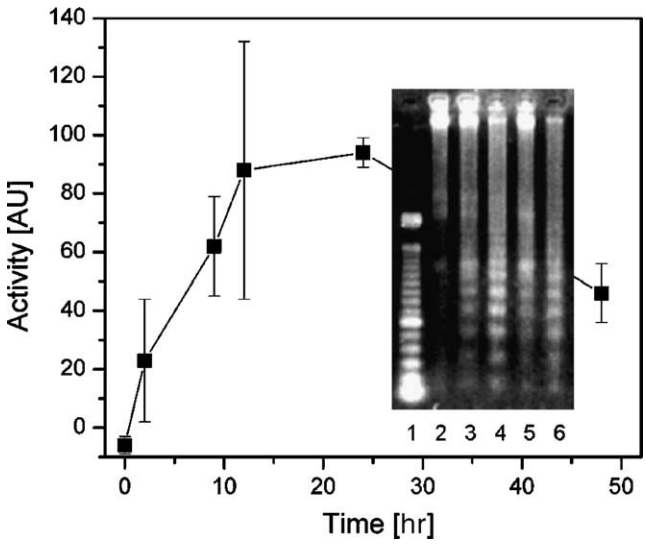

Fig. 5. Disorazol induces an apoptotic process characterized by caspase-3 induction and DNA laddering. U-937 cells showed an increased level of caspase-3 activity with a maximum between 12 and 24 hr after the addition of 10 pg/mL disorazol A_1. The insert shows DNA laddering in the presence of 10 (lanes 3 and 4) or 100 pg/mL (lanes 5 and 6) disorazol A_1 after 24 (lanes 3 and 5) and 48 hr (lanes 4 and 6). Lane 1 shows a standard 100 bp ladder. Lane 2 shows DNA from control cells without disorazol.

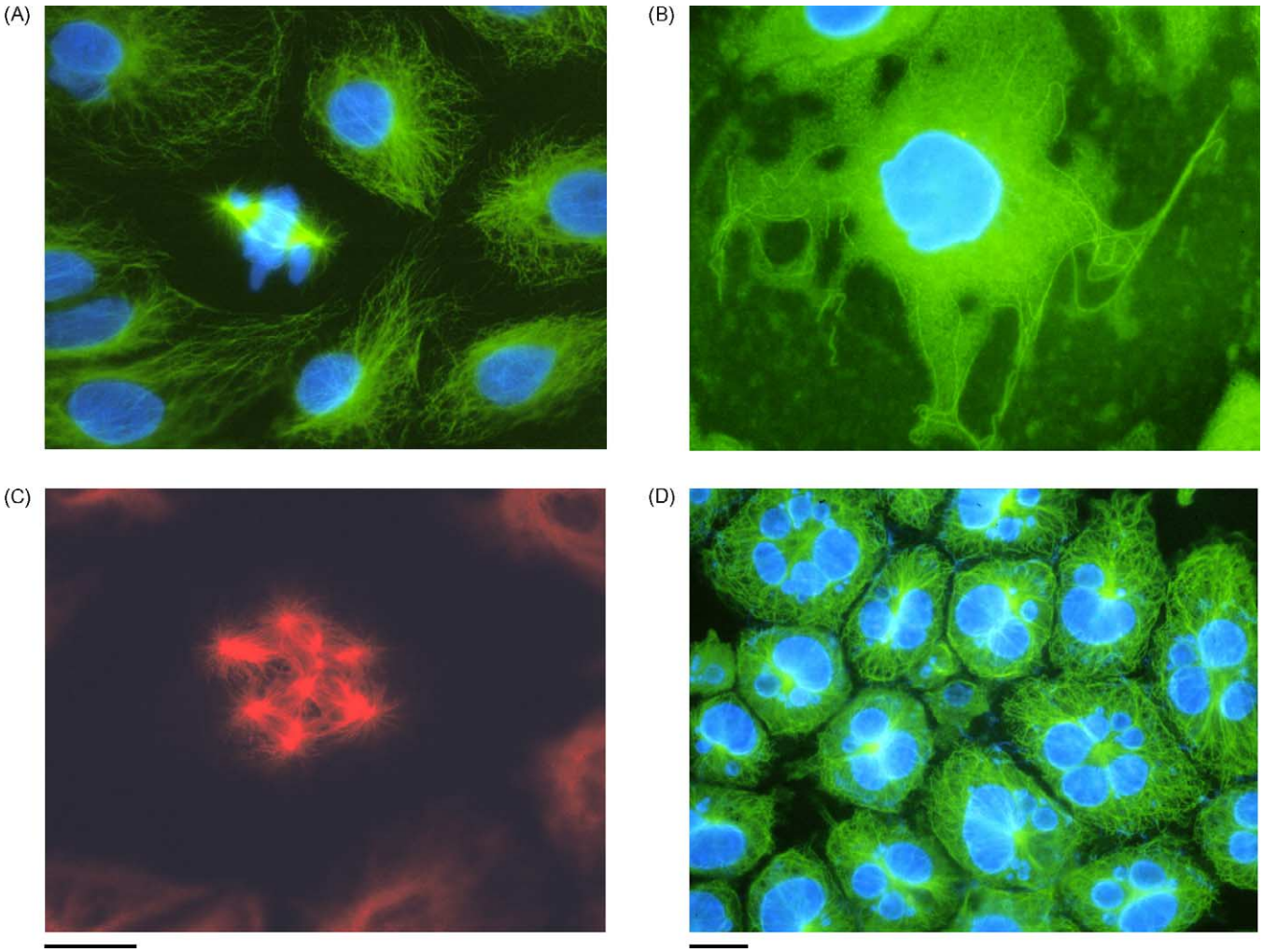

Fig. 6. The action of disorazol A_1 on the microtubules of PtK_2 and L929 cells. Microtubules were labeled green or red; nuclei and chromosomes were stained blue. (A) Untreated PtK_2 cells showing normal microtubules and a bipolar mitotic spindle. (B) Four hours after treatment of the cells with disorazol A_1 (660 pM), the network of the microtubules was completely disrupted. (C) After treatment with low concentrations of disorazol A_1 (13 pM) for 24 hr, mitotic cells showed abnormal spindles with a multipolar configuration. (D) Low concentrations of disorazol A_1 that did not led to a microtubule depletion still induced the formation of multinucleate cells. After 2 days of incubation with disorazol (66 pM) the L929 cells contain nuclei of different size and nuclear fragments. Scale bars: 10 μm (scale bar for panel (C) is also valid for panels (A) and (B)).

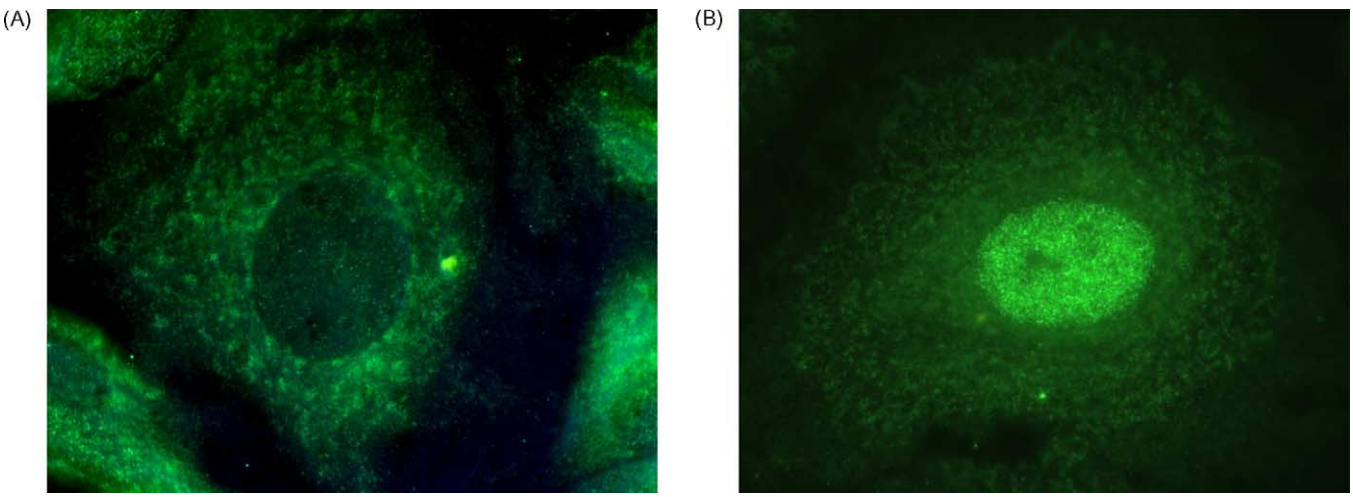

Fig. 7. Low concentrations of disorazol A_1 induce the accumulation of p53 protein in the nucleus of A-549 lung carcinoma cells. (A) Control cells; (B) cells incubated with 13 pM disorazol A_1 for 1 day.

An caspase-3 induction showing a maximum between and 24 hr was also found with KB-3.1 cells (data not shown). To check for DNA cleavage, genomic DNA samples of U-937 cells treated with disorazol A_1 for 24 and 48 hr were separated by electrophoresis on an agarose gel. The inserted image in Fig. 5 shows that disorazol induced DNA ladders after 1 and 2 days.

3.4. Effects on microtubules and p53 localization in cultured cells

Microscopic investigations using immunofluorescence techniques showed that disorazol A_1 interfered with the organization of the microtubular structures in the cells (Fig. 6). The extent of the effect on microtubules was concentration dependent. At drug concentrations of 130 pM and above, the interphase microtubules of PtK_2 cells disappeared within a few hours to within minutes (Fig. 6B). Even after a short incubation period (5 hr), the effect of disorazol A_1 could not be reversed. When the cells were washed and transferred to drug free medium, the microtubular network did not recover. On the other hand, at lower drug concentrations (e.g. 13 pM) only the microtubules of the mitotic spindles seemed to be affected and not the interphase microtubules. The organization and the density of the microtubular network of interphase cells showed no changes in comparison with untreated cells. The mitotic cells showed abnormal spindles with a multipolar configuration (Fig. 6C). The number of the poles varied from three to nine. According to immunofluorescence investigations with antibodies against γ-tubulin and pericentrin, we found that these mitotic cells have only two, seldom four normal MTOCs that contain γ-tubulin and pericentrin, as is the case in centrosomes and spindle poles of normal cells (data not shown).

Low concentrations that did not affect the microtubular network of interphase cells still induced multinucleate cells and an engulfment and fragmentation of nuclei (Fig. 6D).

Treatment of cells with microtubule targeting compounds affects cellular transport, which was clearly shown for the tumor suppressor protein p53 [9]. To assess the effects of disorazol A_1 on p53 localization, A-549 human lung carcinoma cells were treated with low concentrations (13 pM) of the drug. These concentrations had no apparent effect on interphase microtubules, but resulted in enhanced nuclear accumulation of p53 protein (Fig. 7).

3.5. Effect of disorazol A_1 on microtubule polymerization in vitro

As the immunofluorescence studies suggested that disorazol A_1 impairs the formation or the stability of microtubules in the cells, we examined the effect of disorazol A_1 on the polymerization of microtubule protein isolated from porcine brain (Fig. 8). Turbidometric measurements showed that disorazol A_1 inhibited the polymerization of tubulin at substoichiometric doses in a concentration-dependent manner. 1.8 μM of the drug inhibited the polymerization of microtubule protein (10 μM) by 50%, i.e. at a disorazol A_1:tubulin ratio of 0.18. In order to examine the effects of disorazol A_1 on preassembled microtubules, tubulin was polymerized for 15 min. Then disorazol A_1 was added to the microtubules, and their stability was monitored for another 15 min. As shown in Fig. 8, disorazol A_1 induced a depolymerization at substoichiometric concentrations. A drug concentration of 2 μM, i.e. a drug:microtubule protein ratio of 0.2, induced a degradation of 50% of the given microtubules. Thus, the ability of disorazol A_1 to inhibit tubulin polymerization or to induce microtubule depolymerization was nearly the same.

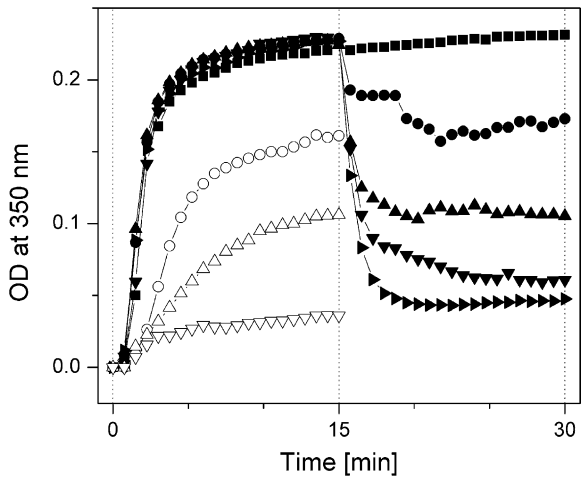

Fig. 8. Influence of disorazol A_1 on microtubule stability and formation *in vitro*. Microtubule proteins (10 μM) were polymerized at 37° for 15 min without disorazol (■). After that, 1 (●), 2 (▲), 3 (▼), and 4 μM (▶) disorazol A_1 were added, and polymerization was monitored at 350 nm for another 15 min. The same experiment was done with disorazol A_1 added from the beginning: (○)1, (△) 2, and (▽) 3 μM.

The effectiveness of disorazol A_1 to inhibit tubulin polymerization *in vitro* was comparable to that of colchicine and vinblastine. A concentration of 1 μM inhibited the polymerization by 25, 20, and 33%, respectively.

We further investigated the effect of disorazol A_1 on the polymerization of microtubule protein by electron microscopy. The control samples (Fig. 9A) showed many microtubules with a normal cylindrical structure, whereas the samples treated with 1 μM disorazol A_1 showed only irregular piles of protein (Fig. 9B). No defined polymeric tubulin structures, like rings or spirals, could be observed. In order to determine whether disorazol A_1 acts directly on tubulin or on associated proteins, we made further electron microscopy investigations using phosphocellulose purified tubulin. In the absence of MAPs, it was necessary to utilize altered reaction conditions that promote microtubule assembly, viz. addition of 0.8 M glutamate at pH 6.6. As

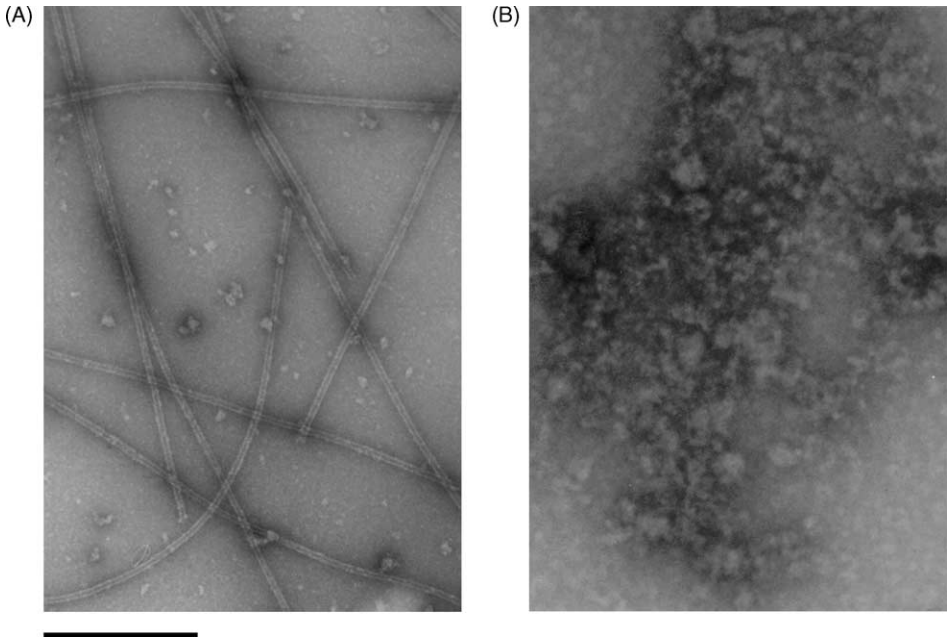

Fig. 9. Electron micrographs of control samples without disorazol showed many microtubules with a normal cylindrical structure (A); scale bar: 1 μm. Samples treated with disorazol A_1 (1 μM) showed only irregular piles of protein (B).

seen with complete microtubule protein, disorazol A_1 induced a degradation of preassembled microtubules also under these conditions. These results indicate that the molecular target of disorazol A_1 is tubulin and not an associated protein.

4. Discussion

During the last few years, several compounds have been isolated from myxobacteria that interfere with the cytoskeleton, either with microfilaments or with microtubules [10–13]. In this report, we demonstrated that disorazol A_1 is a novel antimitotic compound from myxobacteria. After epothilones [10] and tubulysins [13], disorazols are the third class of myxobacterial secondary metabolites that interfere with tubulin polymerization. While epothilone induces the polymerization of tubulin *in vitro* and stabilizes the microtubules in intact cells [14], disorazol A_1, like tubulysin [13], inhibits tubulin polymerization and leads to a depletion of microtubules in intact cells. *In vitro* polymerization assays with microtubule protein as well as electron microscopy investigations with phosphocellulose-purified tubulin demonstrated that disorazol A_1 is an effective inhibitor of tubulin polymerization, and that it acts in a concentration-dependent manner and independently of MAPs, suggesting that disorazol A_1 exerts its effect directly on tubulin rather than on microtubule-associated proteins. Also, it completely depolymerised microtubules prepared *in vitro* without forming rings or similar structures. This suggests that the microtubules are disassembled from their ends. In contrast to other antimitotic agents, disorazol A_1 was equally able to inhibit polymerization of tubulin and to induce depolymerization of microtubules. Phomopsin A, e.g. induces a 50% depolymerization of the microtubules only at concentrations that are 5-folds higher than the concentrations needed to inhibit tubulin polymerization by 50% [15]. The reason for this symmetry of action could be that disorazol A_1 does not induce the formation of tubulin aggregates or ring structures from microtubules, which could raise the light scattering in the polymerization assay.

The immunofluorescence studies of PtK_2 cells that were incubated with very low concentrations (e.g. 13 pM) of the drug showed no significant altering of interphase microtubules. Under these conditions, the number of microtubules was also not detectably decreased. Nevertheless, many nuclei of the treated cells were fragmented. At such low concentrations, disorazol A_1 probably affects only the dynamics of the microtubules without depleting them. Similar observations were made with other antimitotic agents, like *Vinca* alkaloids, which also inhibit the microtubular dynamics at concentrations below those required to inhibit polymerization [16].

The tumor suppressor protein p53 is transported along the microtubules to the nucleus via the minus-end-directed motor protein dynein [17]. The suppression of microtubule dynamics by low concentrations of microtubule targeting compounds was shown to enhance trafficking towards the minus ends of microtubules [9]. Our findings are in agreement with these results. Disorazol A_1 also enhanced the p53 localization in the nucleus at low concentrations that had no apparent effect on interphase microtubules.

But mitotic cells showed abnormal spindles with a multipolar configuration at such low concentrations of disorazol A_1. These were similar to those observed in the presence of tubulysine D [13]. In order to examine whether these structures are organized from a centrosome, we made immunofluorescence stainings using antibodies against γ-tubulin and pericentrin. In most of the mitotic cells with abnormal spindles, only two, seldom four, real microtubule-organizing centers (MTOCs) containing γ-tubulin and pericentrin were observed. These results suggest that the multipolar spindles are not the result of an abnormal centrosome propagation. The few cells with four spindle poles may be hyperploid cells (see below). At higher drug concentrations (>100 pM) the microtubular network of the interphase cells was completely disrupted. The effect of disorazol A_1 was irreversible, which suggests that the compound has a high binding affinity to tubulin.

The mitotic spindle is a highly dynamic molecular machine composed of tubulin, motors and other molecules. It assembles around the chromosomes and distributes them after duplication to the daughter cells. The formation of abnormal spindles let us to suppose that the drug inhibits the proliferation of cells by blocking mitosis. Cell cycle investigations of the treated cells corroborate this assumption. After 24 hr of incubation with disorazol A_1, 85% of U-937 leukemia cells had accumulated in the G_2/M-phase. On the other hand, we observed cells with enlarged nuclei and cells with more than one nucleus after drug treatment. In flow cytometric analyses, we noticed an increasing population of hyperploid cells. Hyperploidy and multinucleate cells can be induced in mammalian cells by other antimitotic agents [18–21]. Microtubule inhibitors, such as nocodazole, colcemid, and taxanes, induce the spindle assembly checkpoint and cause a cell cycle arrest at the M-phase. But after extended exposure to the drugs, the cells begin to enter the G_1-phase without undergoing complete chromosome segregation and cell division, a phenomenon termed mitotic slippage. As a result, the cells undergo DNA rereplication and form hyperploid cells. Disorazol A_1 may induce the hyperploidity of the treated cells by the same mechanism.

Despite the fact that we found clear signs that an apoptotic process is induced by disorazol, most of the cells survive for a longer period of time. L929 mouse fibroblasts were metabolically fully active after an incubation period of 10 days.

Disorazol A_1 has a high inhibitory effects on mammalian cells that include the multidrug-resistant cell line KB-V1 which expresses high Pgp levels. Here disorazol has an advantage over paclitaxel or Vinca alkaloids concerning its application as antitumor drug. Enhanced Pgp expression, leading to enhanced drug efflux and reduced drug accumulation, is a major cause of resistance to both compound groups.

When we compare the *in vitro* and *in vivo* data we find a high difference between the inhibition data found in polymerization assays with purified tubulin and the IC_{50} data obtained with living cells that cannot easily be explained. While the efficacy of disorazol A_1 *in vitro* is comparable to that of other tubulin inhibitors, e.g. vinblastin, it is three orders of magnitude more effective in cells, i.e. the efficacy of disorazol in living cells is much higher than would be deduced from the *in vitro* polymerization experiments. A possible explanation could be that disorazol is accumulated and strongly bound by the cells. This would also explain why the effect of disorazol cannot be stopped by changing the cell culture medium even after a short incubation period. A high accumulation was reported for epothilone B [22]. Though we found that tubulin is a target protein of disorazol, additional modes of action cannot be excluded.

Efforts are made towards a total synthesis of disorazol [23,24] and to develop either a natural or a synthetic derivative as an anticancer drug.

Acknowledgments

We thank Bettina Hinkelmann and Britta Voßwinkel for excellent technical assistance, Maria Höxter for FacScan measurements, and Dr. H. Irschik and Dr. R. Jansen for supplying us with disorazol.

References

[1] Nogales E. Structural insights into microtubule function. Annu Rev Biophys Biomol Struct 2001;30:397–420.
[2] Irschik H, Jansen R, Gerth K, Höfle G, Reichenbach H. Disorazol A, an efficient inhibitor of eukaryotic organisms isolated from myxobacteria. J Antibiot 1994;48:31–5.
[3] Jansen R, Irschik H, Reichenbach H, Wray V, Höfle G. Disorazoles, highly cytotoxic metabolites from the sorangicin-producing bacterium *Sorangium cellulosum*, strain So ce12. Liebigs Ann Chem 1994;1994:759–73.
[4] Mosman T. Rapid colorimetric assay for cellular growth and survival: application to proliferation and cytotoxic assays. J Immunol Methods 1983;65:55–63.
[5] Sloboda RD, Dentler WL, Rosenbaum JL. Microtubules associated proteins and the stimulation of tubulin assembly *in vitro*. Biochemistry 1976;15:4497–505.
[6] Sloboda RD, Belfi LM. Purification of tubulin and microtubule-associated proteins by membrane ion-exchange chromatography. Protein Expr Purif 1998;13:205–9.
[7] Gaskin F, Cantor CR, Schelanski M. Turbidimetric studies of the *in vitro* assembly and disassembly of porcine neurotubules. J Mol Biol 1974;98:737–58.
[8] Thomas H, Coley HM. Overcoming multidrug resistance in cancer: an update on the clinical strategy of inhibiting P-glycoprotein. Cancer Control 2003;10:159–65.
[9] Giannakakou P, Nakano M, Nicolaou KC, O'Brate A, Yu J, Blagosklonny MV, Greber UF, Fojo T. Enhanced microtubule-dependent trafficking and p53 nuclear accumulation by suppression of microtubule dynamics. Proc Natl Acad Sci USA 2002;99:10855–60.
[10] Gerth K, Bedorf N, Höfle G, Irschik H, Reichenbach H. Epothilons A and B: antifungal and cytotoxic compounds from *Sorangium cellulosum* (myxobacteria). Production. J Antibiot 1996;49:560–3.

[11] Gronewold TMA, Sasse F, Lünsdorf H, Reichenbach H. Effects of rhizopodin and latrunculin B on the morphology and on the actin cytoskeleton of mammalian cells. Cell Tissue Res 1999;295:121–9.
[12] Sasse F, Kunze B, Gronewold TMA, Reichenbach H. The chondramides: cytotoxic agents from myxobacteria acting on the actin cytoskeleton. J Natl Cancer Inst 1998;90:1559–63.
[13] Sasse F, Steinmetz H, Heil J, Höfle G, Reichenbach H. Tubulysins, new cytostatic peptides from myxobacteria acting on microtubuli. J Antibiot 2000;53:879–85.
[14] Bollag DM, McQueney PA, Zhu J, Hensens O, Koupal L, Liesch J, Goetz M, Lazarides E, Woods CM. Epothilones, a new class of microtubule-stabilizing agents with a taxol-like mechanism of action. Cancer Res 1995;55:2325–33.
[15] Tönsing EM, Steyn PS, Osborn M, Weber K. Phomopsin A, the causative agent of lupinosis, interacts with microtubules *in vivo* and *in vitro*. Eur J Cell Biol 1984;35:156–64.
[16] Jordan MA, Thrower D, Wilson L. Mechanism of inhibition of cell proliferation by Vinca alkaloids. Cancer Res 1991;51:2212–22.
[17] Giannokakou P, Sackett DL, Ward Y, Webster KR, Blagosklonny MV, Fojo T. p53 is associated with cellular microtubules and is transported to the nucleus by dynein. Nat Cell Biol 2000;2:709–17.
[18] Kung AL, Sherwood SW, Schimke RT. Cell line-specific differences in the control of cell cycle progression in the absence of mitosis. Proc Natl Acad Sci USA 1990;87:9553–7.
[19] Tsuiki H, Nitta M, Tada M, Inagaki M, Ushio Y, Saya H. Mechanism of hyperploid cell formation induced by microtubule inhibiting drug in glioma cell lines. Oncogene 2001;20:420–9.
[20] Brichese L, Valette A. PP1 phosphatase is involved in Bcl-2 dephosphorylation after prolonged mitotic arrest induced by paclitaxel. Biochem Biophys Res Commun 2002;294:504–8.
[21] Abal M, Andreu JM, Barasoain I. Taxanes: microtubule and centrosome targets, and cell cycle dependent mechanisms of action. Curr Cancer Drug Targets 2003;3:193–203.
[22] Lichtner RB, Rotgeri A, Bunte T, Buchmann B, Hoffmann J, Schwede W, Skuballa W, Klar U. Subcellular distribution of epothilones in human tumor cells. Proc Natl Acad Sci USA 2001;98:1743–8.
[23] Hillier MC, Price AT, Meyers AI. Studies on the total synthesis of disorazole C_1: an advanced macrocycle intermediate. J Org Chem 2001;66:6037–45.
[24] Hartung IV, Niess B, Haustedt LO, Hoffmann HMR. Toward the total synthesis of disorazole A_1 and C_1: asymmetric synthesis of a masked southern segment. Org Lett 2002;4:3239–42.